Plant Phenomics 8 (2026) 100165

Contents lists available at ScienceDirect

Plant Phenomics

journal homepage: www.sciencedirect.com/journal/plant-phenomics

Research Article

3D reconstruction analysis of maize-soybean intercropping competition under water stress

Shiming Duan [a,b,c,1], Haochong Chen [a,b,c,1], Shichao Chen [a,b,c,*], Xiangyu Li [a,b,c], Zhenjiang Zhou [d], David Parsons [e], Julianne Oliveira [e], Taisheng Du [a,b,c,**]

[a] State Key Laboratory of Efficient Utilization of Agricultural Water Resources, Beijing, China
[b] National Field Scientific Observation and Research Station on Efficient Water Use of Oasis Agriculture in Wuwei of Gansu Province, Wuwei, 733009, China
[c] Center for Agricultural Water Research in China, China Agricultural University, Beijing, 100083, China
[d] College of Biosystems Engineering and Food Science, Zhejiang University, 310058, Hangzhou, China
[e] Department of Crop Production Ecology, Swedish University of Agricultural Sciences, Umeå, 90183, Sweden

ARTICLE INFO

Keywords:
Maize-soybean intercropping
3D canopy structure
Deficit irrigation
Interplant competition
Water use efficiency

ABSTRACT

Maize-soybean intercropping is a sustainable intensive agroecosystem, though the productivity is constrained by interspecific competition for water and light resources. To enhance the water use efficiency in this intercropping system and understand canopy structure dynamics under the water-limited conditions of arid northwest China, this study proposes a novel optimization strategy that synchronizes deficit irrigation scheduling with crop-specific water requirements during critical phenological phases. Four irrigation regimes were implemented: W1 (full irrigation for both maize and soybean crops), W2 (maize-full and soybean-deficit), W3 (maize-deficit and soybean-full), and W4 (dual deficit). Through UAV-based high-resolution 3D canopy reconstruction ($R = 0.98$ for plant height validation), 14 spatial-geometric descriptors were quantified. The W2 strategy demonstrated superior competitive coordination, enhancing aggressivity of maize (Ams) by 85.9 % through strategic canopy reconfiguration: 11.8 % reduction in maize maximum leaf layer width position (MLLWP), 28.3 % decrease in inter-specific canopy overlap area (COA), and 40.0 % compression of shading convex hull volume (SCHV). These optimized structural adaptations synergistically enhanced photosynthetically active radiation interception (+13.4 %) while achieving concurrent reductions in crop evapotranspiration (ET, −19.7 %) without yield penalty, thereby elevating irrigation water use efficiency (IWUE) by 14.4 % and water equivalent ratio (WER) by 15.9 %. This work provides mechanistic insights into canopy architecture-mediated resource competition mitigation and establishes a technological framework for sustainable intensification in water-limited environments.

1. Introduction

Drought is the main constraint of crop production in arid or semi-arid areas in China, and has been exacerbated by global climate change and population growth [1]. How to utilize limited water and land resources to ensure food security has become a core challenge in 21st-century agricultural development [2]. Improving crop efficiency in resource utilization is not only crucial for unlocking the yield potential of crops but also an important goal for sustainable agricultural development [3]. From a field perspective, crop yield is jointly determined by photosynthetically active radiation (PAR), radiation use efficiency (RUE), and harvest index (HI) [4]. Although HI has approached its theoretical limit through long-term breeding [5], further exploration of yield potential by optimizing PAR and RUE remains a current research topic, and this is closely related to crop morphology and canopy structure [6].

Canopy structure plays a vital role in determining PAR interception (PARi) and crop productivity. In-depth investigation of the mechanisms underpinning the relationship between canopy structure and crop yield production, particularly under conditions of limited water resources, is

* Corresponding author. Center for Agricultural Water Research in China, China Agricultural University, Beijing, China.
** Corresponding author. Center for Agricultural Water Research in China, China Agricultural University, Beijing, China.
E-mail addresses: chenshichaocsc@cau.edu.cn (S. Chen), dutaisheng@cau.edu.cn (T. Du).
[1] These authors contributed equally to this work and should be considered co-first authors.

https://doi.org/10.1016/j.plaphe.2026.100165
Received 30 June 2025; Received in revised form 8 December 2025; Accepted 3 January 2026
Available online 12 January 2026

of significant scientific and practical value [7]. Studies have shown that alternative planting configurations and cultivation management measures can significantly enhance the light interception and utilization efficiency of canopies [8,9]. The maize-soybean intercropping system, due to its unique canopy structure and root distribution, has significant advantages in the utilization of light, heat, water, and soil resources, compared with monoculture systems [10–13]. The tall maize canopy, with its lower extinction coefficient, can transmit more light to the lower soybean canopy, which, with its horizontally arranged leaves and higher extinction coefficient, more fully absorbs the transmitted light [14]. In addition, deep-rooted maize can promote the nitrogen fixation ability of soybean through root exudates [15], as well as better utilize water and nitrogen in the soybean root zone due to interplant root overlap effects [16]. Root overlap can further enhance the canopy advantage of taller crops, though this may lead to intensified interplant competition [17]. Efficient water use in intercropping systems depends mainly on interplant competition and complementarity, which are influenced by crop types, irrigation systems, and spatial arrangements [13,18–20]. By optimizing intercropping strip width and crop planting density, 20–50 % of water and land resources can be saved under limited conditions [21]. Therefore, due to intense competition for light resources, especially in arid regions, the trade-off in water use between crops becomes even more critical [22].

The resource use efficiency in intercropping systems, particularly the enhancement of light interception and utilization efficiency, mainly depends on optimizing the canopy structure of the crop population and fully utilizing interplant complementarity [8,23]. Research has shown that optimizing the canopy extinction coefficient can improve radiation use efficiency by over 26.0 % [24], especially in water-limited environments, making it an effective way to improve intercropping productivity [25]. The extinction coefficient of the canopy changes with the solar zenith angle, which is closely related to leaf extension direction [26]. While geometric light transmission models such as DRT, APSIM, and ERCRT have provided accurate predictions of PARi and exhibited high stability [27,28], traditional models often assume a uniform canopy structure, neglecting the impact of canopy spatial heterogeneity and inter-crop interactions (such as leaf vertical stratification and overlapping), which may lead to biased results [29,30]. Therefore, precise measurement of crop canopy geometric phenotypic characteristics could offer additional insights into the mechanisms of light energy distribution and utilization in crop populations.

Traditional methods of obtaining canopy phenotypic characteristics, such as manual measurements using rulers or telescopic leveling rods, are time-consuming, labor-intensive, and destructive [31]. Recent advancements in high-throughput plant phenotyping technologies have made it possible to monitor crop canopy phenotypic structure and RUE with high precision [32]. By combining high-resolution canopy structural data with intelligent analysis technologies, key factors limiting RUE and their regulatory mechanisms can be explored in depth [33]. For instance, 3D reconstruction of individual crops and small populations using multi-view geometry methods (SFM-MVS) in field environments not only provides an accurate reflection of crop growth but also enables precise quantification of plant interactions [34]. Canopy geometric features extracted from 3D point cloud data (such as canopy volume, surface area, plant height, and maximum leaf width) can further reveal the dynamic patterns of interplant competition and resource allocation [35–38]. Studies on maize-soybean intercropping systems have shown that 3D point cloud data generated by drones can be used to analyze the impact of canopy height differences, row orientation, and latitude on light interception and shading, providing theoretical support for optimizing intercropping system design [39–42].

Although previous studies have focused on optimizing intercropping canopy structures through adjustments in planting density, sowing time, and row orientation [21,43,44], research combining irrigation strategies and variety selection to further optimize canopy structure and enhance light interception under water scarcity conditions is lacking. Existing 3D modeling studies have shown that this technology significantly improves the accuracy of crop yield and light interception predictions, while revealing differences in light energy utilization across different planting systems. However, exploration of interplant relationships, canopy spatial structure characteristics, and their water regulation mechanisms in intercropping systems has not yet been fully explored. This study aims to use drones and high-throughput 3D modeling technology to analyze the dynamic impact of canopy heterogeneity on resource use efficiency under deficit irrigation conditions. The specific objectives include: (a) quantifying the relationship between canopy competition space and resource use efficiency in intercropping systems; (b) elucidating how water regulation and plant morphology influence spatial heterogeneity within the plant canopy.

2. Materials and methods

2.1. Field experiments

Field experiments were conducted from May to October 2023 at the Gansu Wuwei Oasis Agricultural Water Use Efficiency National Field Science Observation and Research Station (37°52′ N, 102°50′ E, elevation 1581 m). This region has a continental temperate arid climate, receiving approximately 3000 h of sunshine annually. Annual evaporation and precipitation in the region are 2000 mm and 164 mm, respectively. During May to October 2023, the effective precipitation measured was 73.6 mm. The daily average radiation reached up to 29.07 MJ m^{-2}, and from June onwards, the daily average radiation consistently exceeded 25 MJ m^{-2} (Fig. S1).

The experiment utilized two maize varieties with distinct morphologies: a compact type (M1, Xianyu 335) and a spreading type (M2, Longdan 4), along with a single shade-tolerant soybean variety, Longhuang 3(S). Four different water treatments were applied in the maize-soybean intercropping system: M1S-W1 and M2S-W1, where both maize and soybean were fully irrigated throughout the growing season; M1S-W2 and M2S-W2, where maize was fully irrigated throughout its growing season, and soybean received deficit irrigation (50 % I) from germination to flowering (VE to R1) and from the grain-filling to maturity stages (R6 to R7); M1S-W3 and M2S-W3, where soybean was fully irrigated throughout its growing season, and maize received deficit irrigation (50 % I) from germination to jointing (VE to V14) and from the grain-filling to maturity stages (R3 to R4); M1S-W4 and M2S-W4, where both maize (VE to V14 and R3 to R4) and soybean (VE to R1 and R6 to R7) received deficit irrigation (50 % I). For monoculture maize, the varieties M1 and M2 were subjected to full irrigation throughout their entire growth period under treatments M1-W1 and M2-W1, as well as regulated deficit irrigation (VE to V14 and R3 to R4, 50 % I) under treatments M1-W4 and M2-W4. In the case of monoculture soybean, full irrigation was applied for the entire growth period under treatment S-W1, while deficit irrigation (VE to R1 and R6 to R7, 50 % I) was implemented under treatment S-W4. Irrigation amounts during the experiment are shown in Table 1.

The water requirement calculation formula for the fully irrigated treatment [45] is:

$$I = K_c \times \sum_{i=1}^{n} ET_{0i} - EP \quad (1)$$

Where, K_c is the crop coefficient. For maize the values are 0.7 (VE-V14), 1.15 (VT-R3), and 0.5 (R3-R4). For soybean, the values are 0.5 (VE-R1), 1.15 (R1-R5), and 0.5 (R6-R7). ET_{0i} represents the reference crop evapotranspiration on the i-th day within a given irrigation period, calculated using the Penman–Monteith formula [46], in mm. EP is the effective precipitation during the irrigation period, in mm.

The irrigation method used was drip irrigation with film mulching, with the film retained until harvest. Each plot measured 23.03 m^2 (4.9 m × 4.7 m). Each treatment had three replicates. Sowing was

Table 1
Irrigation amounts and frequencies per treatment and growth stage.

Planting Pattern	Treatment	Maize Irrigation amount and Frequency (mm/times)			Soybean Irrigation amount and Frequency(mm/times)			Total Irrigation(mm)
		VE-V14	VT-R3	R3-R4	VE-R1	R1-R5	R6-R7	
Intercropping	M1S-W1, M2S-W1	163.4/3	101.0/4	93.2/2	136.8/3	70.0/4	86.7/2	651.1
	M1S-W2, M2S-W2	163.4/3	101.0/4	93.2/2	87.4/3	70.0/4	43.4/2	558.4
	M1S-W3, M2S-W3	100.7/3	101.0/4	46.6/2	136.8/3	70.0/4	86.7/2	541.8
	M1S-W4, M2S-W4	100.7/3	101.0/4	46.6/2	87.4/3	70.0/4	43.4/2	449.1
Monoculture	M1-W1, M2-W1, S-W1	163.4/3	101.0/4	93.2/2	158.8/3	70.0/4	86.7/2	357.6, 156.7
	M1-W4, M2-W4, S-W4	100.7/3	101.0/4	46.6/2	109.4/3	70.0/4	43.4/2	248.3, 113.4

performed with fixed row spacing, and intercropping followed a "2 + 3+2 + 3″ pattern, with crops planted in rows oriented east-west. The row spacing for maize was 40 cm, with a plant spacing of 12 cm, and for soybean, the row spacing was 30 cm, with a plant spacing of 16 cm. The inter-row spacing between maize and soybean was 70 cm (Fig. S2). For monocultures, the row and plant spacing for maize and soybean were consistent with those used in the intercropping system. Fertilization for maize included 260 kg ha^{-1} of nitrogen (N), 45 kg ha^{-1} of P_2O_5, and 36 kg ha^{-1} of K_2O – 30 % of nitrogen was applied as basal fertilizer, 60 % at the V14 stage, and 10 % at the R3 stage. For soybean, fertilization included 78 kg ha^{-1} of nitrogen, 45 kg ha^{-1} of P_2O_5, and 36 kg ha^{-1} of K_2O as basal fertilizer. Field management practices (e.g., fertilization and weed and pest control) were implemented to maximize the yield according to local practices. Specifically, maize at the V14 stage was sprayed with pyrethroid to control aphids, and abamectin was applied to soybean at the R1 stage to control red spider mites.

2.2. Canopy 3D reconstruction, phenotypic extraction, and accuracy validation

2.2.1. Canopy image acquisition and 3D reconstruction

At four growth stages – maize V10-soybean R1, maize VT-soybean R3, maize R2-soybean R5, and maize R4-soybean R7 – images were captured using the RGB sensor of the DJI Phantom 4 RTK UAV system (SZ DJI Technology Co. Ltd., China). Photographs of field crop canopies were taken between 09:00 and 10:00 on a clear morning using orthophoto and cross-circling oblique, setting the flight altitude to 4 m above the overall canopy each time [47], which effectively prevented canopy disturbance from UAV rotor airflow (Fig. 1a). The method by which the flight path was established is referred to in Xiao [47]. Based on the captured images, Agisoft Metashape (Agisoft LLC, St. Petersburg, Russia; version 1.7.0) was used for 3D point cloud reconstruction (Fig. 1). This software is one of the mainstream tools utilizing the SFM (Structure from Motion-Multi-View Stereo) algorithm for point cloud generation. The

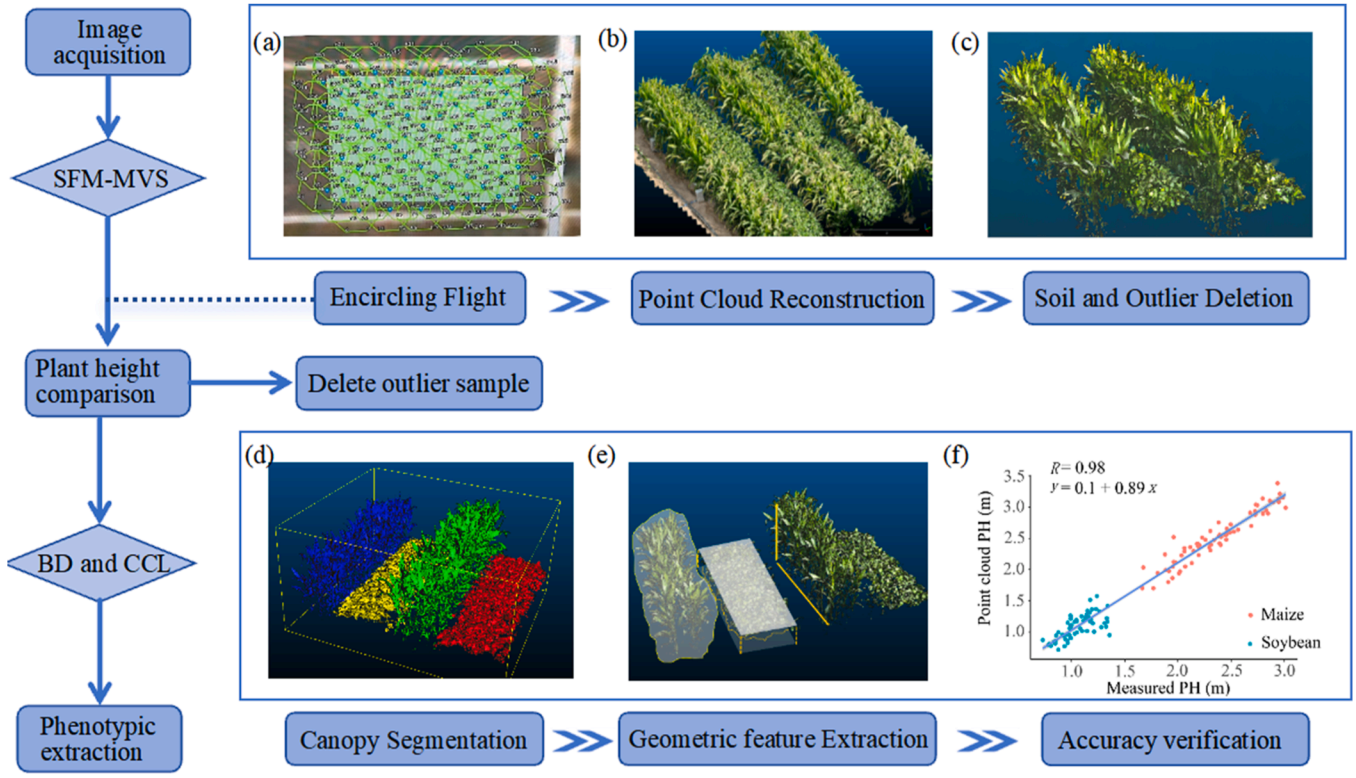

Fig. 1. Canopy phenotypic feature extraction and accuracy validation
(a) Schematic path trajectories of the images obtained using orthophoto and cross-circling oblique; (b) 3D point cloud of the canopy obtained from the multi-view image reconstruction; (c) sifting of soil from the canopy point cloud; (d) segmentation of the corn and soybean point clouds within a single plot using the BD and CCL algorithms; (e) extraction of the corn and soybean phenotypes; (f) correlation analysis between the measured plant height values of maize and soybean and the extracted point cloud values.

process includes image matching, sparse point cloud generation, and dense point cloud reconstruction. Statistical outlier removal filter was applied to remove noise. To enhance computational efficiency, voxel-based downsampling was used with a voxel size of 0.003 m. Finally, in CloudCompare (2.13.0, http://www.cloudcompare.org/), manual segmentation was performed to obtain the point clouds for each maize/soybean trial plot.

2.2.2. Vegetation point cloud extraction

In each plot (23.03 m^2), plant and soil point clouds were initially segmented (Fig. 1c). The point cloud that was generated contains RGB three-channel color information. The vegetation index is calculated (as in Eqs. (2)–(7)), with a threshold of 25 to segment the soil and crop point clouds for deriving the final color-coordinate moments (COM) [48].

$$ExG = 2 * G - R - B \tag{2}$$

$$ExR = 1.4 * R - G \tag{3}$$

$$ExGR = ExG - (1.4 * R - G) \tag{4}$$

$$CIVE = 0.441 * r - 0.811 * g + 0.385 * b + 18.78745 \tag{5}$$

$$VEG = \frac{g}{r^{a} * b^{1-a}} \tag{6}$$

$$COM = 0.25 * ExG + 0.30 * ExGR + 0.33 * CIVE + 0.12 * VEG \tag{7}$$

where R, G, and B represent the red, green, and blue components of each pixel, and r, g, and b are the normalized R, G, B values, respectively.

2.2.3. Soybean and maize point cloud segmentation

Point cloud processing was conducted using the open-source CloudComPy (https://github.com/CloudCompare/CloudComPy), with the specific process including the extraction of the upper canopy and the segmentation of point clouds for soybean and maize (Fig. 1). The point cloud was divided into 100 segments based on vertical height, and the vertical distribution profile of the point cloud quantity for each segment was generated. Due to the distribution characteristics of the soybean/maize canopy, the upper canopy of maize, being the primary light interception part, had a higher point cloud density. The first high-frequency zone was observed in the upper canopy. From the height of this high-frequency zone to above the soybean canopy, the point cloud density continuously decreased until it increased again at the soybean canopy height, forming a new high-frequency zone. Based on the vertical distribution characteristics of the soybean/maize intercropping point clouds, a bimodal distribution (BD) algorithm using histograms was applied to detect the lowest frequency zone between the two high-frequency zones, which was considered the canopy height threshold. Point clouds above this threshold correspond to the maize canopy, while those below the threshold represent both the soybean canopy and the lower maize point clouds (Fig. S3).

Connected-component labeling (CCL) is a computer vision algorithm that segments the selected cloud into smaller parts, each separated by the minimum distance. Each part is a connected component (i.e., a group of "connected" points). CloudComPy uses a 3D grid to extract connected components. This grid is derived from an octree structure, where the minimum gap between two components can be defined at the octree level. The CCL algorithm was applied to the point cloud below the threshold, with the octree level set to 9 when the soybean canopy was far from the maize canopy in the early growth stages, and set to 10 or 11 when the two canopies were closer in the later stages. This method effectively segmented the point clouds of soybean and maize. The maize lower canopy point cloud obtained from the segmentation was then merged with the maize canopy point cloud extracted in the previous step, successfully obtaining the point clouds of the two crops in the soybean/maize intercropping system (Fig. 1d).

2.2.4. Parameter extraction and validation

This study extracted seven crop canopy geometric parameters and seven system canopy geometric parameters from the 3D point cloud images of the maize-soybean intercropping system (Fig. 1e and Table 2) to evaluate the structure and function of the intercropping system. The system canopy geometric parameters include Canopy Overlap Area (COA), Shading Convex Hull Volume (SCHV), Shading Leaf Volume

Table 2
Definition and calculation methods of canopy parameters.

Metric (Abbreviation)	Description	Calculation Method
Plant Height (PH)	The height of maize or soybean plants.	Determined as the maximum z-axis value of the point cloud for an individual plant.
Canopy Volume (CV)	The volume of maize or soybean canopies.	Generated by voxelizing the point cloud into a surface model, multiplying the number of voxels by their unit volume.
Canopy Projected Area (CPA)	The projected area of maize or soybean canopies.	Calculated using a grid-based statistical method on the point cloud's projection.
Canopy Coverage (CC)	The coverage rate of maize or soybean canopies within the study area.	The ratio of the convex hull area of the maize or soybean point cloud to the total study area.
Maximum Leaf Layer Width Position (MLLWP)	The position of the maximum leaf layer width at a specific height.	Determined by layering the point cloud by height and identifying the height of the layer with the maximum projected area.
Projected Convex Hull Area (PCHA)	The projected convex hull area of maize or soybean canopies.	Computed by projecting the point cloud onto the x-y plane and calculating the convex hull area.
Convex Hull Diameter (CHD)	The maximum convex hull diameter of maize or soybean canopies.	Calculated using the rotating calipers method to find the maximum pairwise distance on the convex hull.
Canopy Overlap Area (COA)	The overlapping area of maize and soybean canopies.	Computed as the intersection area of the convex hulls of maize and soybean point clouds on the x-y plane.
Shading Convex Hull Volume (SCHV)	The convex hull volume of maize shading soybean (higher maize points over soybean).	Determined by selecting maize points above soybean height and calculating the 3D convex hull volume.
Shading Leaf Volume (SLV)	The leaf volume of maize shading soybean (higher maize points over soybean).	The algorithm groups points within the maize-shaded soybean region based on spatial proximity, and the identified cluster volumes are summed to obtain the SLV.
Leaf to Convex Hull Volume Ratio (LVPM)	The percentage of maize leaf volume relative to the convex hull volume.	The ratio of maize shading leaf volume (SLV) to the shading convex hull volume (SCHV).
Maximum Direct Sunlight Width of Soybean (MSWS)	The maximum width of soybean exposed to direct sunlight.	Computed as the maximum width in the y-axis direction of the soybean region unshaded by maize.
Unshaded Area of Soybean (UAS)	The area of soybean canopy not shaded by maize leaves.	Calculated as the area of the soybean polygon after subtracting the maize convex hull.
Leaf Edge Distance (LED)	The distance from the outermost edge of maize leaves to the soybean canopy.	Measured as the vertical (z-axis) height difference between the outermost edge of maize leaves (above the soybean canopy) and the soybean canopy.

(SLV), Leaf to Convex Hull Volume Ratio (LVPM), Maximum Direct Sunlight Width of Soybean (MSWS), Unshaded Area of Soybean (UAS), and Leaf Edge Distance (LED). The crop canopy geometric parameters include Plant Height (PH), Canopy Volume (CV), Canopy Projected Area (CPA), Canopy Coverage (CC), Maximum Leaf Layer Width Position (MLLWP), Projected Convex Hull Area (PCHA), and Convex Hull Diameter (CHD).

2.3. Field measured data

2.3.1. Canopy light interception

Beginning 49 days after sowing, PARi was measured approximately every 15 days, with additional measurements taken before and after irrigation. Observations were made between 11:30 a.m. and 2:00 p.m. on clear, sunny days, using the AccuPAR Plant Canopy Analyzer (LP-80, METER Company, USA). Measurements were taken for the incident PAR at the canopy top (20 cm above the canopy), at the bottom of the maize rows, between the maize and soybean inter-rows, and at the bottom of the soybean rows. PARi is the difference between the PAR at the canopy top and the PAR at the canopy bottom. The PARi of intercropping system was calculated as the weighted average of light interception per unit area for both crops:

$$PAR_i = PAR_{si} \times A_s + PAR_{mi} \times A_m \tag{8}$$

where, PAR_{mi} andPAR_{si} represent the light interception (μmol $m^{-2}s^{-1}$) for intercropped maize and soybean, respectively. A_m andA_s represent the land area proportions of intercropped maize and soybean per hectare, with maize at 0.45 and soybean at 0.55.

2.3.2. Shoot biomass and yield

Biomass was destructively sampled and measured after the completion of the UAV aerial photography. Three representative plants with uniform growth were selected from each plot for destructive sampling. Plant height and maize leaf angle were measured, and the stems, leaves, and fruits were placed in paper bags. The samples were then oven-dried at 105 °C for 2 h for deactivation and at 85 °C until a constant weight was reached. The shoot biomass was weighed using an electronic scale with 0.01 g precision.

When maize and soybean reached full maturity, grain yield was measured in the intercropping and monoculture plots. The measurement area for maize was 3.2 m^2 (4 m × 0.8 m), and for soybean, it was 3.6 m^2 (4 m × 0.9 m). After harvest, the grain was manually threshed, and yields were adjusted for moisture content of 14.0 % for maize and 13.5 % for soybean. The total yield of an intercropping system is calculated as the sum of the yields of intercropped maize and intercropped soybean per unit area [49]:

$$Yield = Y_{si} + Y_{mi} \tag{9}$$

where, Y_{mi} and Y_{si} are the grain yields (kg ha^{-1}) for intercropped maize and soybean, respectively, corresponding to 45 % and 55 % of the land area per hectare.

2.3.3. Intercrop relative competitiveness and nutrient competition ratio

The aggressivity (A_{ms}) and competitive ratio (CR_{ms}) of the intercropping system were calculated based on yield [50]:

$$A_{ms} = \frac{Y_{mi}}{(Y_{mm} \times A_m)} - \frac{Y_{si}}{(Y_{ms} \times A_s)} \tag{10}$$

$$CR_{ms} = [Y_{mi}/Y_{mm} \times A_m]/[Y_{si}/Y_{ms} \times A_s] \tag{11}$$

Where, Y_{mm} and Y_{ms} represent the grain yields for monoculture maize and soybean (kg ha^{-1}). When $A_{ms} > 0$, $CR_{ms} < 1$, it indicates that soybean is more competitive than maize. When $A_{ms} < 0$, $CR_{ms} > 1$, it indicates that maize is more competitive than soybean.

2.3.4. Irrigation water use efficiency and water use efficiency

Irrigation Water Use Efficiency (IWUE, kg m^{-3}) is the ratio of grain yield to the system irrigation amount during the growing season. The calculation formula is as follows:

$$IWUE = \frac{Yield}{I} \times 0.1 \tag{12}$$

where, I is represent the total irrigation amount (mm) during the growing season for intercropping system, respectively.

Water Use Efficiency (WUE, kg m^{-3}) is the ratio of grain yield to the system evapotranspiration (ET) during the growing season. The calculation formula is as follows:

$$WUE = \frac{Yield}{ET} \times 0.1 \tag{13}$$

Crop water consumption (ET, mm) is estimated using a simplified water balance method:

$$ET = EP + I - (W_{t_2} - W_{t_1}) + G - R - D \tag{14}$$

where, ET-crop water consumption (mm); EP-rainfall (mm); G-groundwater recharge (mm); I-irrigation amount (mm); R-surface runoff (mm); D-deep drainage (mm); W_{t_1} and W_{t_2} are soil water storage in the 0–100 cm soil layer at the beginning and end of the experiment respectively (mm). Due to the deep groundwater depth (>40 m), flat terrain, low rainfall and shallow infiltration depth under drip irrigation, G, R and D were ignored and the equation was simplified as:

$$ET = EP + I - (W_{t_2} - W_{t_1}) \tag{15}$$

Specimens were obtained at 10-cm depth intervals to a maximum depth of 100 cm, systematically collected from a single sampling location within each plot. The collected samples were oven-dried at 105 °C for 48 h to assess soil gravimetric water content.

2.3.5. Land equivalent ratio and water equivalent ratio

The Land Equivalent Ratio (LER) and Water Equivalent Ratio (WER) are calculated using the following formulas [51]:

$$LER = \frac{Y_{mi}}{Y_{mm}} + \frac{Y_{si}}{Y_{ms}} \tag{16}$$

$$WER = \frac{WUE_{mi}}{WUE_{mm}} + \frac{WUE_{si}}{WUE_{ms}} \tag{17}$$

where, WUE_{mi} and WUE_{mm} are the water use efficiencies for intercropped and monoculture maize, respectively. WUE_{si} and WUE_{ms} are the water use efficiencies for intercropped and monoculture soybean.

3. Statistical analysis

Pearson correlation analysis was used to examine the linear relationship between the measured plant heights of maize and soybean and the point cloud-derived plant heights to validate the accuracy of the point cloud extraction. Pearson correlation analysis was also applied to examine the linear relationships between the phenotypes, while the Mantel test was used to explore relationships between phenotypes and observed productivity, inter-crop relationships, and resource utilization ratios.

An Elastic Net Regression model was used to select important features. First, the coefficient matrix of the Elastic Net model was extracted as a sparse matrix, and non-zero coefficients were filtered to identify explanatory variables that have a significant contribution to the response variable. Linear regression models were then constructed using the selected important features. Key statistics, including the coefficient of determination (R^2) and the significance levels of the coefficients, were obtained from the model summary. Model performance was assessed using statistical indicators such as Root Mean Square Error (RMSE) and the coefficient of determination (R^2).

$$R^2 = \frac{\sum_{i=1}^{n} (\hat{x}_i - \bar{x})^2}{\sum_{i=1}^{n} (x_i - \bar{x})^2} \quad (18)$$

$$RMSE = \sqrt{\frac{\sum_{i=1}^{n} (\hat{x}_i - x_i)^2}{n}} \quad (19)$$

where, $\hat{x}_i$ represents the point cloud-estimated productivity parameters, competitiveness parameters, and resource utilization equivalents, while x_i denotes the measured values, $_i$ is the sequence of the samples, and n is the sample size. A Fisher's one-way analysis of variance (ANOVA) with a minimum significant difference test ($p < 0.05$) was conducted to assess the significance of differences in canopy phenotypic parameters, productivity indicators, inter-species competition indicators, and resource utilization equivalents under deficit irrigation. The mean values and standard deviations of the traits were calculated.

Data processing, feature selection, modeling, and result analysis were all performed using custom scripts developed in R version 4.3.2. Using these methods, this study accurately identified the features that significantly impact the target variables, developed an efficient regression model, and validated the model's predictive ability and robustness through various evaluation criteria. This provides reliable statistical support for data-driven biological phenotypic analysis.

4. Results

4.1. Accuracy validation and correlation analysis of 3D canopy phenotypic traits

Point cloud-derived Plant height (PH) and field-measured data points demonstrated strong concordance with the regression line and exhibited an excellent fit ($R = 0.98$), validating the validity and precision of the point cloud extraction methodology (Fig. 1f). The BD-CCL combined method demonstrated significant advantages in ensuring the accuracy of main structural segmentation for both crops (Fig. S4). The phenotypic characteristics of maize and soybean canopies demonstrate a statistically significant interspecific complementarity correlation (Fig. 2). Of the maize canopy phenotypic parameters, Projected convex hull area (PCHA) and Convex hull diameter (CHD) displayed the most robust positive associations with productivity metrics, including biomass accumulation and yield. In contrast, Canopy projected area (CPA) and Canopy volume (CV) of soybean exhibited the strongest positive correlations with analogous productivity metrics. PCHA and CPA of Maize, PCHA of soybean exhibited highly significant positive correlations with parameters associated with interspecific competitive capacity. PH, CPA, PCHA, and MLLWP of maize demonstrated significant positive associations with the manifestation of intercropping resource utilization efficiency (LER and WER). Furthermore, systemic indices including Shading convex hull volume (SCHV) and Canopy overlap area (COA) demonstrated highly significant positive correlations with both canopy parameters of the two species; these indices similarly displayed strong correlations with productivity metrics. The system-level COA, SCHV, Shading leaf volume (SLV), and PARi exhibited varying degrees of significant positive correlations.

4.2. Generalized analysis of the importance of canopy spatial geometric phenotypes for intercropping system characteristics

Systematic evaluation of canopy spatial geometry parameters (Fig. 3) revealed critical functional associations in intercropping systems. Maize PCHA demonstrated superior predictive capacity for both interspecific competitive dominance and population productivity, attaining the highest important feature coefficients: 0.64 for yield prediction, 0.47 for Ams, and 0.62 for CRms. COA emerged as the most influential determinant for CRms ($\beta = 0.73$). Maize CPA exhibited peak

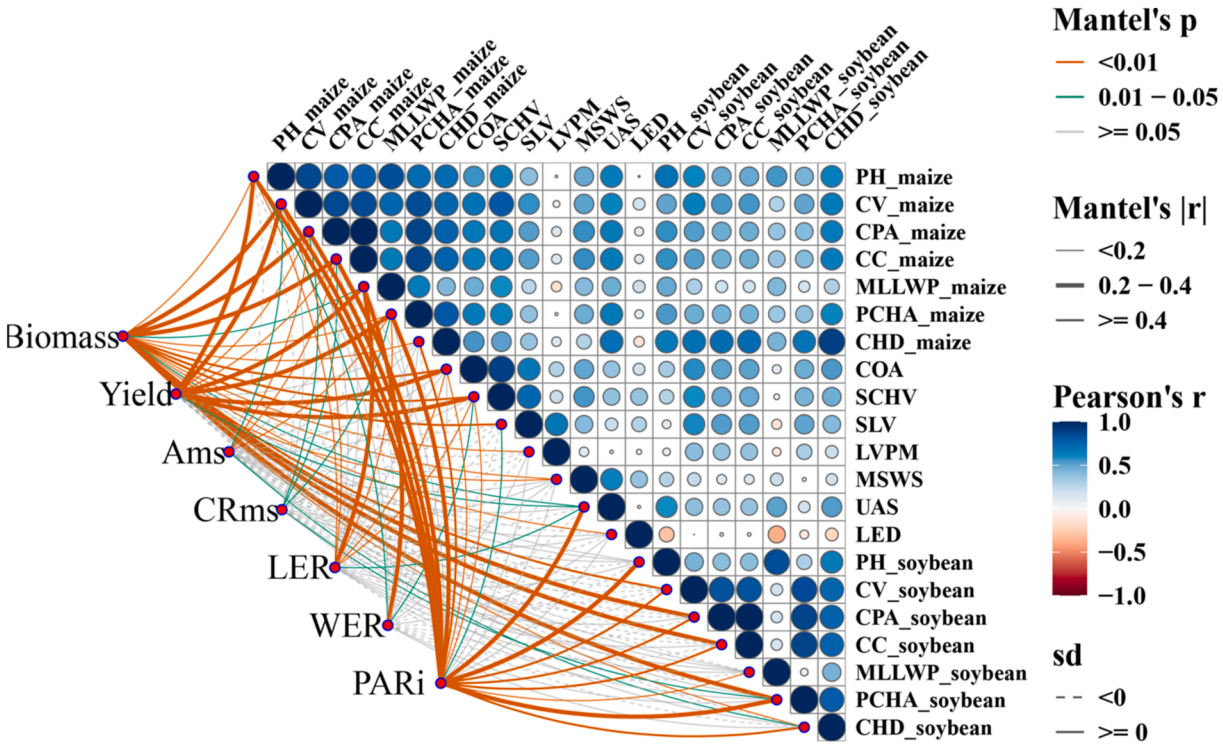

Fig. 2. Correlation analysis between 3D-model-derived phenotypic traits and crop productivity related parameters of maize and soybean.
The heatmap displays the Pearson correlation coefficients (r) between variables, with colors ranging from −1 (blue for negative correlation) to +1 (red for positive correlation). The color of the connecting lines indicates the significance of the Mantel test (p-value): orange for $p < 0.01$, green for $0.01 \leq p < 0.05$, and gray for $p \geq 0.05$. The thickness of the lines corresponds to the absolute value of the Mantel correlation coefficient, with thicker lines indicating stronger correlation. The line types differentiate the signs of the correlation coefficients (controlled by the "sd" variable), with solid lines representing $r \geq 0$ and dashed lines representing $r < 0$.

explanatory power for LER (β = 0.48) and WER (β = 0.52), while SCHV contributed substantially to WER prediction (0.50). Notably, MLLWP dominated PARi at system level (β = 0.57).

4.3. Analysis of canopy geometric parameters

The PCHA, CPA, MLLWP, and PH of different maize varieties exhibit consistent trends across growth stages (Fig. 4), showing a pattern where full irrigation (W1) consistently outperforms deficit irrigation (W2, W3 and W4) treatments. W1 outperformed all other treatments across all growth stages. The W2 treatment in the intercropping system with deficit irrigation displayed larger values for PCHA, CPA, MLLWP, and PH compared to W3 and W4. The PCHA for the W2 treatment was 12.5 % higher than other deficit treatments ($p > 0.05$), while CPA was 13.1 % higher ($p > 0.05$). MLLWP was 28.8 % higher ($p < 0.05$), and PH was 16.8 % higher than other treatments ($p < 0.05$).

From the genotypic perspective, under full irrigation treatment, the PCHA and CPA values of M1 were consistently lower than M2 across all developmental stages ($p > 0.05$), with an average decrease of 8.1 %. Under water deficit conditions, M1 had 4.0 % and 5.2 % lower values than M2 during the V10 and R2 growth phases, respectively. However, during the VT and R4 stages, M1 had greater values surpassing M2 by

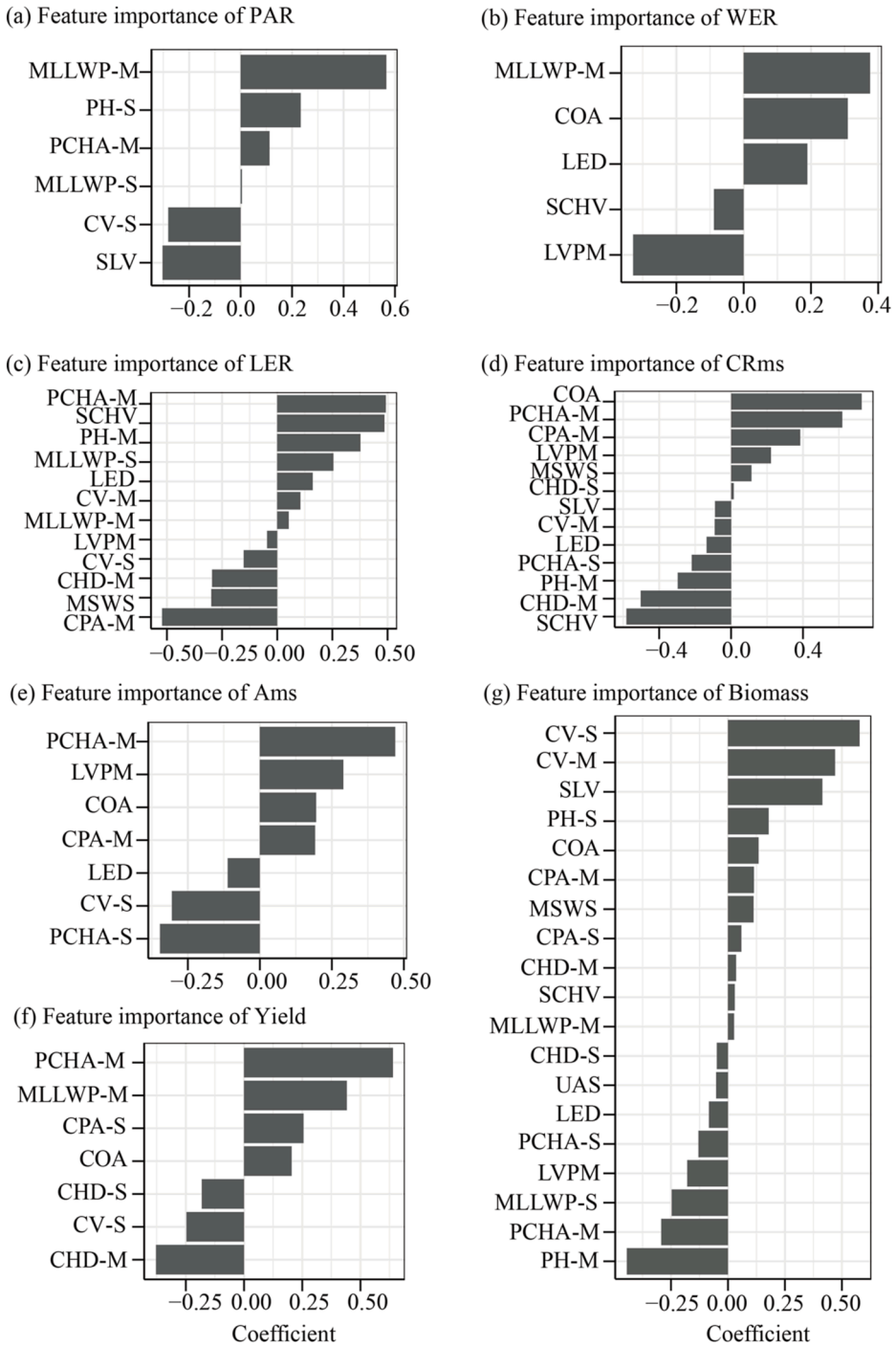

Fig. 3. The important features selected by the elastic net regression model
a, b, c, d, e, f, and g, correspond to the following variables in intercropping systems: PAR interception, water equivalent ratio (WER), land equivalent ratio (LER), competitiveness (Ams), competition ratio (CRms), yield, and biomass.

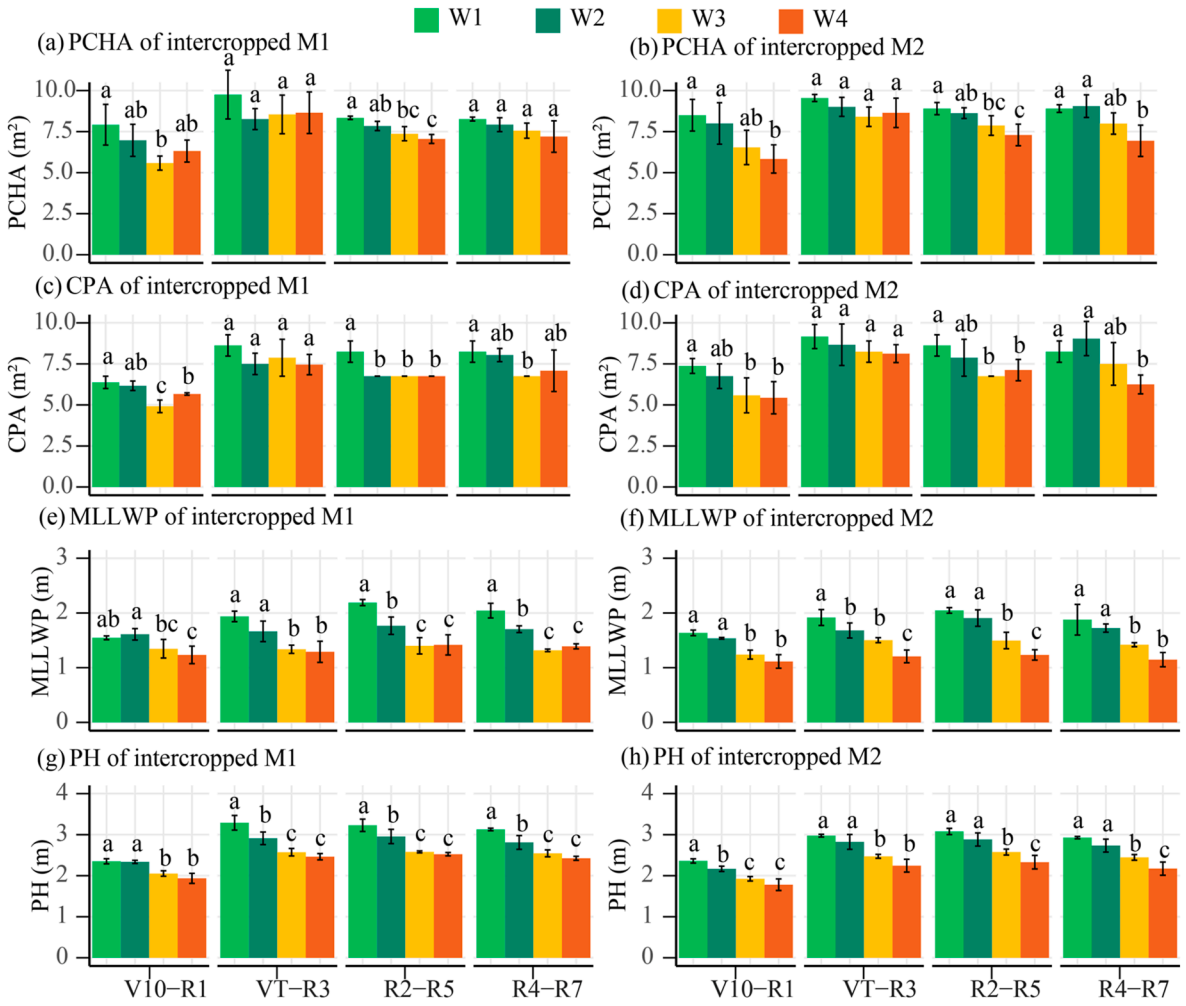

Fig. 4. Canopy geometric parameters of maize under different treatments
(a) and (b) correspond to the Projected Convex Hull Area (PCHA) of intercropped M1 and M2, (c) and (d) correspond to the Canopy Projected Area (CPA) of intercropped M1 and M2, (e) and (f) correspond to the Maximum Leaf Layer Width Position (MLLWP) of intercropped M1 and M2, and (g) and (h) correspond to the Plant Height (PH) of intercropped M1 and M2. Different letters indicate significant differences between irrigation treatments during the same growth period, with a significance level of $p < 0.05$.

5.7 % and 8.4 %. Regarding plant height (PH), M1 was consistently taller than M2 under identical water treatments, with an average enhancement of 5.6 % throughout the complete growth cycle ($p < 0.05$). The maximum leaf layer width position (MLLWP) displayed varietal divergence across water treatments, with M2 exhibiting 2.9 % higher values than M1 under W2 and W3 conditions, whereas M1 outperformed M2 by approximately 7.0 % in W1 and W4 treatments ($p < 0.05$).

For CV of Soybean (Fig. 5), W2 had higher values in the early stages and W3 was higher in the later stages. During the R1 and R3 stages, the W3 treatment had the lowest soybean CV, lower than other treatments by 10.2 % ($p < 0.05$). By the R7 stage, the W3 treatment had the highest rate of increase in CV, exceeding others by 90.5 % ($p < 0.05$). Among the deficit irrigation treatments, the W2 treatment had the highest soybean CV, which was on average 8.2 % higher than other treatments ($p > 0.05$). Genotypic analysis revealed soybean intercropped with M1 maize cultivars demonstrated greater CV than those paired with M2 under equivalent water treatment. Specifically, under full irrigation, the

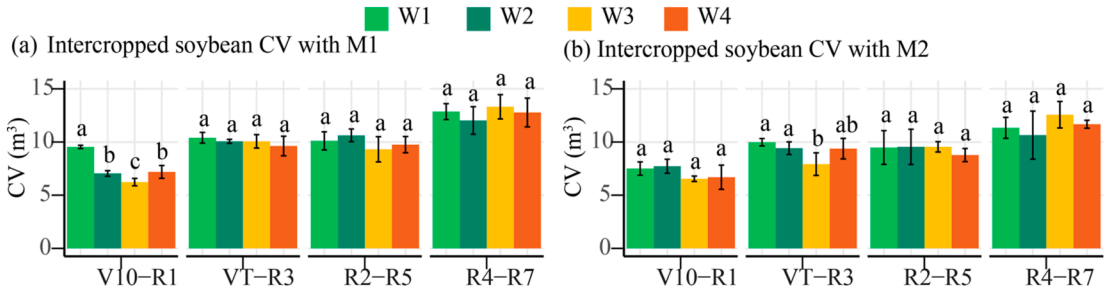

Fig. 5. Canopy volume (m^3) of intercropped soybean under different treatments
Different letters represent significant differences between irrigation treatments at the same growth stage at the $p < 0.05$ level.

CV was increased by 9.5 % ($p < 0.05$), while under deficit irrigation, it was increased by 6.7 % ($p > 0.05$).

SCHV and COA exhibited a general trend of W1 > W2 > W3 > W4 across all growth stages (Fig. 6). Specifically, the COA under the W2 treatment was significantly lower than under the W1 treatment by 23.2 %, 51.3 %, and 30.6 % in the V10, VT, and R4 stages, respectively. SCHV was significantly lower than W1 by 9.7 %, 11.8 %, and 4.7 % in the V10, VT, and R2 stages but was significantly higher than W3 and W4 treatments by 65.3 % and 103.9 % ($p < 0.05$).

4.4. Field-measured data

4.4.1. Productivity indicators, competition indices, and resource utilization efficiency indices

Biomass and yield consistently had a ranking of W1>W2>W3>W4 across cultivars under varying water regimes (Fig. 7a–b). The W2 treatment exhibited the lowest reduction rates among the deficit irrigation treatments, with a 5.68 % decrease in biomass ($p < 0.05$) and a 4.46 % decrease in yield ($p > 0.05$). Additionally, W2 outperformed the other deficit treatments (W3 and W4) by 12.1 % and 12.4 % ($p < 0.05$), respectively. Genotypic analysis indicated M1S surpassed M2S in yield under W3 (+5.0 %, $p < 0.05$) and biomass under W1 (+1.9 %, $p > 0.05$), while M2S was generally greater than other treatments with 6.1 % higher yield ($p < 0.05$).

Ams and CRms had a ranking of W2>W1>W4>W3 (Fig. 7c–d), with Ams>0 across all treatments. Notably, W3 approached competitive equilibrium (Ams≈0, CRms<1), while W2 had 85.9 % greater Ams and 39.3 % greater CRms than other treatments. Ams of M2 genotypes were 108.3 % and 49.4 % greater than M1 in well-watered intercrops (W1 and W2), contrasting with M1's 16.0 % greater Ams under deficit irrigation (W3 and W4).

All treatments had LER and WER >1 (Fig. 7e–f). W3 had 14.1 % higher LER than W2 and W4 ($p < 0.05$), while W1 had 16.0 % lower WER than deficit treatments. M1 had 3.1 % greater LER in water-stressed intercrops (W3 and W4), with greater WER (23.3 %) evident only in W4.

4.4.2. The ET, WUE, and IWUE of intercropping system

Compared to the W1 treatment, ET under all deficit irrigation treatments decreased by 21.9 %, with treatment hierarchy W2>W4>W3 (Table 3). The W3 treatment demonstrated exceptional water conservation, reducing ET by 26.5 % (M1) and 22.3 % (M2) relative to other regimes. There were differences between maize genotypes – M1 had 39.8 % higher ET than M2 under identical water management ($p < 0.05$).

WUE (Table 3) peaked under W3 for both cultivars – M1 was 16.75 % greater and M2 was 20.4 % greater than other treatments. While M1 systems showed no significant WUE variations across irrigation regimes, M2 was 24.3 % greater in W2 versus W1. Notably, M2 consistently had greater (30.48 %) WUE than M1 under matched irrigation conditions.

W1 was the treatment with the lowest IWUE – M1 and M2 cultivars under W1 were 6.8 % and 17.2 %, respectively, compared to their efficiency under other water treatments. In contrast, W2 had optimal IWUE for both cultivars, 14.15 % greater than W1. Notably, there was no difference in IWUE between M1 and M2 under identical water management conditions.

4.4.3. Trends in PARi

As shown in Fig. 8, the PARi within maize-soybean inter-row spaces and intercropping system exhibited a consistent hierarchy across irrigation treatments: W1 > W2 > W3 > W4. Specifically, the W2 treatment increased PARi by 10.6 % and 13.9 % compared to W3 and W4, respectively. Temporal analysis revealed that PARi in W2 converged with W1 after 98 days, a trend particularly pronounced in the M2 system. The W1 treatment reached its maximum PARi earlier (85 days after sowing, 1859 μmol $m^{-2}s^{-1}$), whereas W2 had a later peak in PARi (1684 μmol $m^{-2}s^{-1}$ at 98–110 days), indicating extended light-energy utilization during late reproductive stages.

Genotypic comparisons under identical water regimes showed that M2 intercropping systems had 4.7 % higher inter-row PARi and 9.7 % greater system PARi than M1 across the entire growth period.

5. Discussion

5.1. Coupling mechanism between canopy geometry and resource use efficiency

Crop canopy geometric parameters significantly affect the efficient utilization of resources such as water, soil, light, and heat by modulating multi-dimensional mechanisms including light interception, temperature regulation, and ventilation [52]. Complex, multi-layered, and heterogeneous canopy architectures are considered to optimize the capture and distribution of solar radiation, enhance the use of diffuse light, and ultimately increase yield [53]. Studies have shown that greater plant height (PH) facilitates a more stratified vertical distribution of leaves, thereby enhancing photosynthetic capacity and cooling [54]. Similarly,

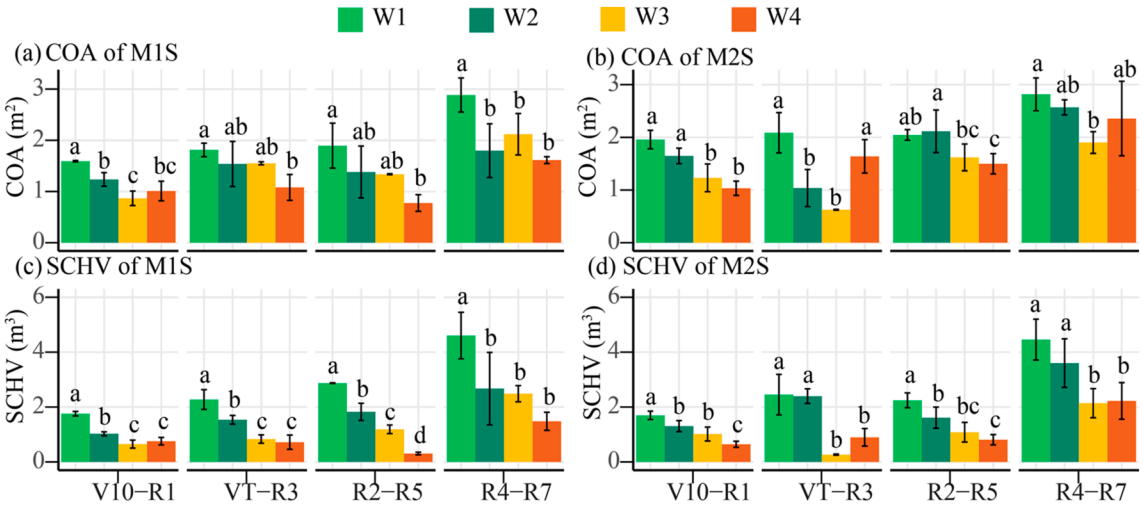

Fig. 6. Canopy geometric parameters of system under different treatments
(a) (a) and (b) correspond to the Canopy Overlap Area (COA) of M1S and M2S, while (c) and (d) correspond to the Shading Convex Hull Volume (SCHV) of M1S and M2S. Different letters represent significant differences between irrigation treatments at the same growth stage at the $p < 0.05$ level.

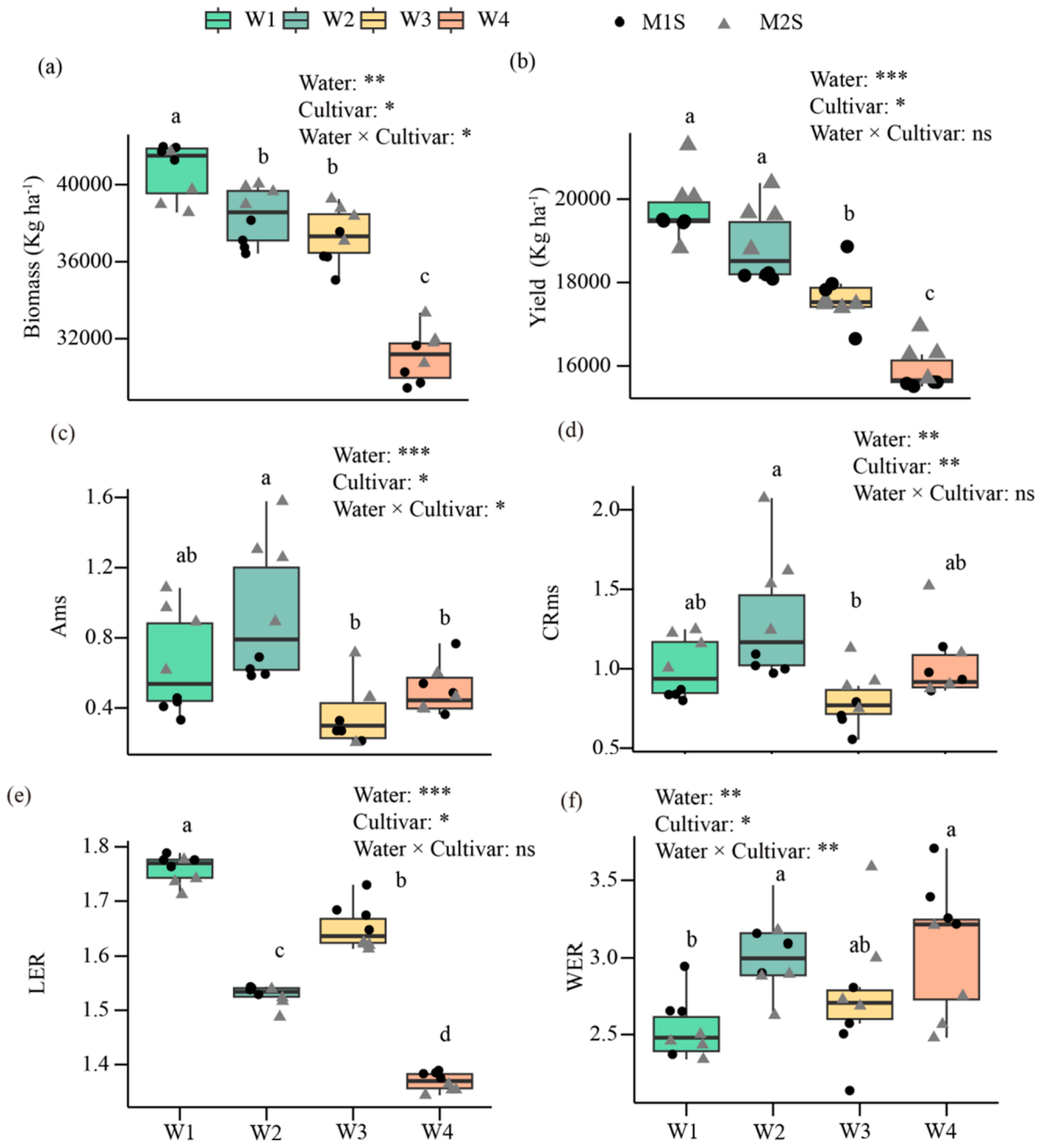

Fig. 7. Productivity, interspecies competitive relations, and resource utilization equivalents under different treatments
(a) biomass, (b) yield, (c) aggressivity (Ams), (d) competitive ratio (CRms), (e) Land equivalent ratio (LER), and (f) water equivalent ratio (WER) under different treatment in the intercropping system. Different letters represent significant differences between irrigation treatments at the $p < 0.05$ level. "*", "**" and "***" indicate statistically significant differences at $p < 0.05$, $p < 0.01$, and $p < 0.001$, respectively.

Table 3
ET, WUE and IWUE for intercropping populations under different irrigation treatments.

Treatment	ET (mm)	WUE (Kg m^{-3})	IWUE (Kg m^{-3})
M1S-W1	476.0 a	5.0 cd	7.6 bc
M1S-W2	475.0 a	4.6 d	8.3 abc
M1S-W3	342.9 b	5.8 bcd	7.4 c
M1S-W4	350.5 b	5.4 bcd	8.6 ab
M2S-W1	340.0 b	6.7 b	7.3 c
M2S-W2	286.0 cd	8.3 a	9.1 a
M2S-W3	242.6 d	8.6 a	7.7 bc
M2S-W4	307.7 bc	6.3 bc	8.9 a

the position of the maximum leaf layer width (MLLWP) reflects the stratification of canopy structure and corresponds to the height at which the plant most effectively captures light [55]. By adjusting leaf layer distribution, canopy structure can mitigate self-shading and promote competition for light resources within the community [56]. Under drought stress, plants may shift the MLLWP closer to the ground to reduce transpirational water loss [57].

In this study, both MLLWP and PH of maize exhibited a highly significant positive correlation with PARi (Fig. 2). Deficit irrigation under intercropping significantly reduced maize PH and MLLWP (Fig. 4); however, under the W2 treatment, these values were 16.8 % and 28.8 % higher than those under the other deficit irrigation treatments, leading to an 11.4 % increase in maize PARi. Moreover, the horizontal

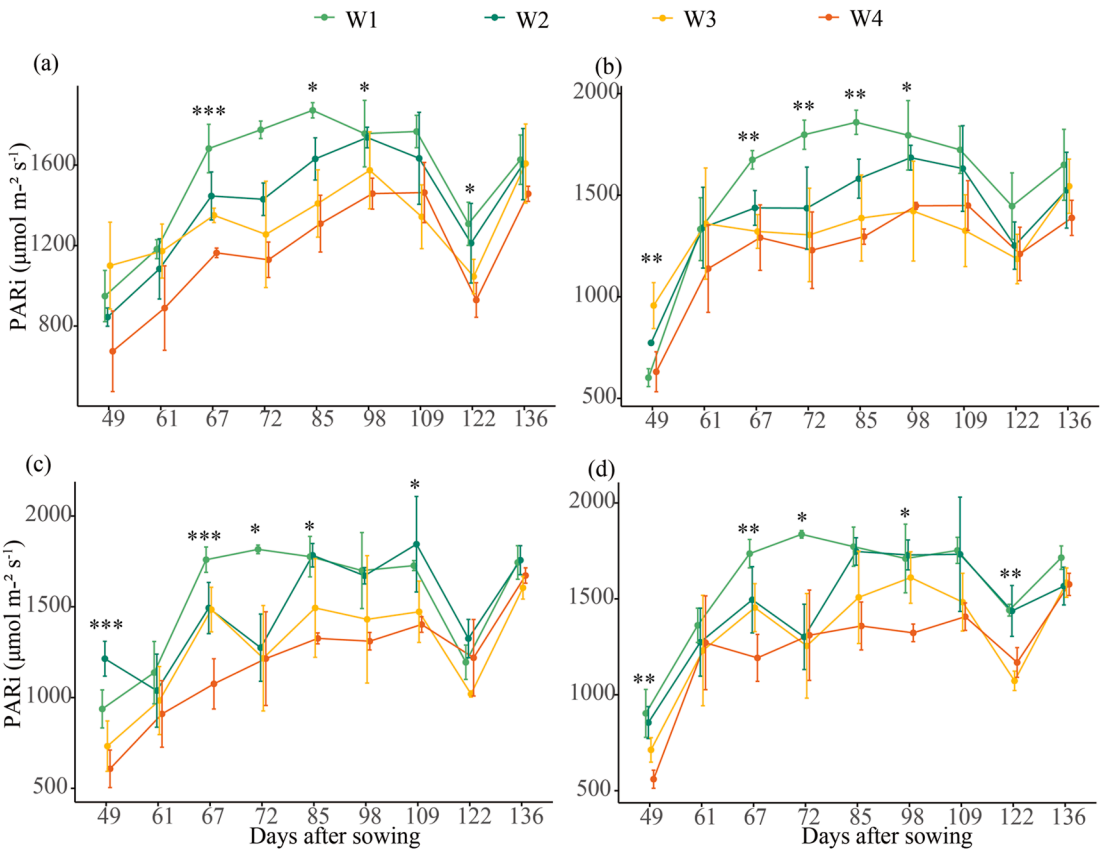

Fig. 8. Changes in PARi between maize-soybean inter-row and intercropping system under different treatments
(a) PARi trends of M1S in the inter-row, (b) PARi trends of M1S in the intercropping system, (c) PARi trends of M2S in the inter-row, (d) PARi trends of M2S in the intercropping system. "*", "**" and "***" indicate statistically significant differences at $p < 0.05$, $p < 0.01$, and $p < 0.001$, respectively, between deficit irrigation treatments (W2, W3, W4) and conventional irrigation (W1) in the intercropping system.

heterogeneity of canopy structure can increase the spatial occupation of the canopy, enabling more light to be intercepted by leaves at different heights and positions, thereby reducing ground-level light loss and facilitating the maintenance of diversity and the differentiation of ecological niches [58,59]. However, some studies have indicated that vertically stratified species play a dominant role in light distribution, while horizontal heterogeneity influences the overall pattern of light distribution [8,60]. This study is the first to confirm this theory in a maize–soybean intercropping system.

Canopy projection area (CPA) and canopy volume (CV) are important indicators for evaluating horizontal heterogeneity and the effective photosynthetically active area [61]. Although there were no significant differences in CPA among deficit-irrigated maize treatments, the significant advantages in PH and MLLWP, together with the stable CV of soybean (Fig. 5), resulted in the PARi of the intercropping system in the W2 treatment being 12.2 % higher than that of the W3 and W4 treatments. Additionally, canopy biomass and yield were increased by 12.1 % and 12.4 % (Table. S 1), respectively. More importantly, the projected convex hull area (PCHA) of maize and the CV of soybean in the W2 treatment were comparable to those in W1, while total irrigation volume was reduced by about 16.6 %, leading to an increase in IWUE by 12.2 % (Table. S 1).

Although there is a strong correlation between crop canopy geometric parameters and resource use efficiency, the underlying mechanisms in intercropping systems become considerably more complex due to pronounced interspecific leaf interweaving, overlapping, and spatial heterogeneity in leaf distribution [62,63]. This study innovatively considered the effects of interspecific canopy structural interactions on resource utilization in maize–soybean intercropping systems. The results indicated that shaded convex hull volume (SCHV) and canopy overlap area (COA) are key indicators for demonstrating the advantages of maize–soybean intercropping (Figs. 2 and 3). Compared with full irrigation for both maize and soybean, deficit irrigation during non-critical growth stages significantly reduced SCHV and COA in the intercropping system (Fig. 4). The W2 treatment exhibited the most pronounced improvement in water use for intercropping, with the WER increasing by 15.9 % and the IWUE increasing by 14.4 %. Notably, SCHV and COA in the W2 treatment were 82.6 % and 19.7 % higher than those in other deficit irrigation treatments, indicating that minimizing interspecific competition is not always the optimal strategy for improving resource use efficiency. There exists a trade-off between canopy structure and resource utilization at the system level.

However, in the multiple regression analysis, the linear models fitted between canopy structure and the predicted values of LER and WER showed relatively weak correlations (Fig. S5), indicating that resource use efficiency may also be influenced by the root-zone environment. Previous studies have shown that the spatial distribution and competition of interspecific roots, along with their morphological plasticity, synergistically enhance land and water use efficiency, deep-rooted maize and shallow-rooted soybean achieve spatial niche separation and temporal asynchrony in peak resource demand, thereby facilitating coordinated competitive–complementary interactions [64]. Moreover, maize root exudates (such as flavonoids) can promote nitrogen fixation nodulation in soybean, further strengthening nitrogen uptake and utilization in maize [65]. Therefore, under deficit irrigation, resource use efficiency in maize-soybean intercropping systems is jointly regulated by canopy and root-zone interactions.

5.2. Effects of canopy heterogeneity on interspecific relations and intercropping benefits

Canopy heterogeneity modulates resource allocation among crops, thereby promoting interspecific complementarity, mitigating competition, and enhancing both land use efficiency and the overall benefits of intercropping systems [44]. However, some studies have suggested that the implementation of agronomic practices such as reduced nitrogen fertilization, widening row spacing, and increased planting density, which moderately intensify the coordination of interspecific competition, can further augment the benefits of intercropping systems [66–68]. In this study, maintaining adequate irrigation for maize combined with regulated deficit irrigation for soybean (W2) significantly enhanced the interspecific advantage of maize, with Ams and CRms being 85.9 % and 39.3 % higher than other treatments (Fig. 7c and d), whereas yields exhibited no significant differences compared to W1 (Fig. 7a). This is because the yield advantage of the maize–soybean intercropping system primarily depends on the increase in kernel number per ear of maize [66]. In this study, the kernel number per ear of maize under W2 was 9.5 % higher than that under W3 and W4 (Table. S 1). Furthermore, analysis of crop phenotypes showing high correlation with interspecific competition parameters revealed that the proposed indices, SCHV and COA are the main factors influencing interspecific relationships (Fig. 3). Reduced leaf overlapping led to higher PAR transmission from the maize canopy to the soybean canopy and a more uniform light distribution [69], facilitating stable soybean yields under water stress. With full irrigation in maize, the MLLWP, PCHA, and COA values were higher by 36.5 %, 119.0 %, and 36.6 % respectively compared to deficit irrigation, which enhanced interspecific advantages. Concurrently, the leaf angle decreased by 11.9 %, reducing the shading effect on soybean. As a result, the PARi of the soybean canopy increased by 12.9 %, contributing to more stable yield and improved resource use efficiency.

This study also found that excessive suppression of the dominant crop's competitiveness can lead to uneven light distribution, thereby negatively impacting both light distribution and overall crop yield. Under the W3 treatment, deficit irrigation applied to maize resulted in a 30.88 % decline in Ams and a 24.31 % reduction in the CRms (Fig. 7c and d), as well as a 22.34 %–26.53 % decrease in ET. However, this also increased the maize leaf angle by 12.3 %, intensified shading on soybean [70], reduced PARi by 14.7 %, and ultimately led to a 15.1 % decrease in maize yield. Given that maize contributes the most to total yield in the intercropping system, system yield was reduced by 12.0 %. Therefore, future studies should focus on more precisely balancing irrigation management and interspecific competition to further enhance the benefits of intercropping systems.

Furthermore, under root-zone water scarcity in maize, interspecific competition is primarily mediated through light interception [22]. Compact-type maize cultivars in intercropping systems demonstrate more efficient resource partitioning compared to sprawling-type cultivars, thereby mitigating competitive pressures on soybean [21]. First, compact maize exhibits enhanced xylem embolism resistance under water stress [71], enabling better canopy acclimation to moisture deficits and reduced canopy mortality risk [72]. Their erect leaf architecture minimizes leaf overlap, improving both photosynthetic efficiency and water productivity [72]. Second, the concentrated root spatial distribution of compact maize allocates more soil volume for soybean development [73], thereby strengthening competitive capacity of soybean (Fig. 7). Consequently, compact-type (M1) maize-soybean intercropping systems under deficit irrigation demonstrated greater interspecific complementarity and superior LER compared to spreading-type (M2) counterparts.

5.3. Management implications of variety selection and irrigation strategy

In arid or water-limited environments, regulated deficit irrigation enhances light interception efficiency and canopy photosynthesis by adjusting canopy structural parameters, such as reducing leaf angle, shortening internode length, and decreasing leaf area index [74,75], thereby promoting sustainable agricultural production without significant yield penalties. Structural analysis of crop canopies can be used for analysis and understanding of regulated deficit irrigation using 3D point clouds. The use of sensors such as RGB or Lidar enables rapid access to a certain number of crop canopies. The point cloud structure provides researchers with a method to quantitatively analyze the canopy structure, such as the newly proposed SCHV in this paper, which is a phenotypic indicator that could not be measured before. Additionally, the shooting method employed in this paper necessitates only an RGB UAV, a technology that is comparatively more economical than utilizing Lidar. Conversely, the present study exclusively employed point cloud data, which can be integrated with multispectral and thermal imaging to facilitate a more comprehensive analysis of intercropping deficit irrigation in the future. In this study, both PCHA of maize and CV of soybean exhibited significant correlations with yield (Fig. 2), corroborated by high-fidelity multivariate regression models for biomass ($R^2 = 0.93$) and yield ($R^2 = 0.73$) prediction (Fig. S4).

Within maize-soybean intercropping systems, shading from maize leaves redistributes PAR in soybean canopies. COA and SCHV show strong explanatory power for both PARi and productivity (Fig. 2). Soybean partially counteracts maize shading through compensatory CV expansion (Fig. 5), reducing row-zone canopy overlap [76], and enhancing light distribution homogeneity, thereby improving PARi interception and yield stability. Notably, deficit irrigation in intercropping systems significantly reduced COA and SCHV (Fig. 6), with W2 displaying minimal reduction and achieving the highest system yield (+12.4 %), indicating that moderate shading contributes to yield stability.

In maize-soybean intercropping systems, maize yields significantly surpass soybean monoculture, and the LER is predominantly driven by maize productivity [20]. Full irrigation of maize ensures yield stability in intercropping systems. Although spreading type maize-soybean intercropping increases COA and SCHV, intensifying shading effects on soybean, the concurrent enhancement of system PARi (Fig. S5) partially offsets shading-induced yield losses. Maize deficit irrigation significantly reduces group COA and SCHV, weakening the competitive advantage of maize. However, decreased maize PCHA and CV impair light competition capacity, resulting in a 17.9 % maize yield reduction (Table S1) and overall system productivity decline. Remarkably, under maize deficit-soybean full irrigation conditions, M1 intercropping systems outperformed M2 by 2.0 % in yield, demonstrating that W3-treated compact maize-soybean intercropping configurations exhibit superior drought adaptability under water scarcity.

5.4. Future research directions

While this study clarifies the relationship between canopy architecture and resource utilization in maize-soybean intercropping systems under water deficit, several critical areas require further investigation:

(a) Integrated Modeling Frameworks: Combining 3D point cloud-derived canopy structural optimization models with process-based crop growth simulators could enhance predictive accuracy for crop productivity and enable data-driven precision agriculture.
(b) IoT-Enhanced Resource Management: Implementing IoT networks for real-time monitoring of soil moisture dynamics and field microclimates, coupled with 3D phenotyping, may quantify interspecies interactions, mitigate competition, and optimize light/thermal/water/soil resource allocation for intelligent irrigation scheduling.

6. Conclusions

This study integrates UAV-based remote sensing with high-throughput 3D modeling to mechanistically resolve how water-regulated canopy architecture governs interspecific relationships and resource use efficiency in a maize-soybean intercropping system. We established a predictive framework linking canopy geometry, cultivar selection, and irrigation strategy to productivity optimization in precision agriculture. Key conclusions are as follows:

(a) Interspecific Competition and Resource Complementarity: Moderate interspecific competition promotes resource use efficiency, particularly under the full-irrigated maize and deficit-irrigated soybean strategy, which significantly improves irrigation water use efficiency (IWUE) and water equivalent ratio (WER).
(b) Canopy Geometric Traits and Resource Efficiency: System canopy geometric parameters, particularly shading leaf convex hull volume (SCHV) and canopy overlap area (COA), critically influence light-use efficiency in intercropping systems. Structural optimization through fine-tuning canopy projected convex hull area (PCHA) and canopy volume (CV) effectively enhances crop productivity and irrigation water efficiency under water-limited conditions.
(c) Cultivar Selection and Irrigation Strategy: Cultivar compatibility and irrigation protocols significantly affect system-level resource efficiency. Compact maize-soybean configurations demonstrate superior drought resilience under water scarcity. While the deficit-irrigated maize and full-irrigated soybean strategy reduces canopy overlap and shading volume to improve water use efficiency (WUE), it concurrently decreases total light interception and yield, highlighting the necessity for optimal irrigation scheduling.

Author contributions

Shiming Duan: Conceptualization, Visualization, Writing-original paper. Taisheng Du: Designed the research, Conceptualization, Supervision. Shichao Chen: Conceptualization, Writing-revise paper, Supervision. Haochong Chen: Analyzed the data. Zhenjiang Zhou: Conceptualization, Writing-revise paper. David Parsons: Conceptualization, Writing-revise paper. Julianne Oliveira: Conceptualization, Writing-revise paper. Xiangyu Li: Visualization.

Data availability

The source code used in this study is available for noncommercial use and the code can be downloaded from https://github.com/Pepe-oss/3D-Reconstruction-analysis-of-maize-soybean-intercropping-competition-under-water-stress. The data of this study are available from the corresponding author upon request.

Conflict of interests

The authors declare that they have no competing interests.

Acknowledgments

This work was supported by National Key R&D Program of China (No. 2022YFD1900503) and the National Natural Science Foundation of China (52239002 and 52209072).

Appendix A. Supplementary data

Supplementary data to this article can be found online at https://doi.org/10.1016/j.plaphe.2026.100165.

References

[1] J.S. Wallace, Increasing agricultural water use efficiency to meet future food production, Agric. Ecosyst. Environ. 82 (1–3) (2000) 101–119.
[2] D.K. Ray, N. Ramankutty, N.D. Mueller, et al., Recent patterns of crop yield growth and stagnation, Nat. Commun. 3 (2012) 1293, https://doi.org/10.1038/ncomms2296.
[3] L. Rong, K. Gong, F. Duan, et al., Yield gap and resource utilization efficiency of three major food crops in the world–A review, J. Integr. Agric. 20 (2) (2021) 349–362.
[4] R.M. Gifford, J.H. Thorne, W.D. Hitz, et al., Crop productivity and photoassimilate partitioning, Science 225 (4664) (1984) 801–808.
[5] R.T. Furbank, W.P. Quick, X.R.R. Sirault, Improving photosynthesis and yield potential in cereal crops by targeted genetic manipulation: prospects, progress and challenges, Field Crops Res. 182 (2015) 19–29.
[6] L. Cabrera-Bosquet, C. Fournier, N. Brichet, et al., High-throughput estimation of incident light, light interception and radiation-use efficiency of thousands of plants in a phenotyping platform, New Phytol. 212 (1) (2016) 269–281.
[7] G.W. Van Esse, The quest for optimal plant architecture, Science 376 (6589) (2022) 133–134.
[8] R. Wang, Z. Sun, W. Bai, et al., Canopy heterogeneity with border-row proportion affects light interception and use efficiency in maize/peanut strip intercropping, Field Crops Res. 271 (2021) 108239.
[9] R.A. Slattery, D.R. Ort, Perspectives on improving light distribution and light use efficiency in crop canopies, Plant Physiol. 185 (1) (2021) 34–48.
[10] Y. Hong, N. Heerink, M. Zhao, et al., Intercropping contributes to a higher technical efficiency in smallholder farming: evidence from a case study in gaotai county, China, Agric. Syst. 173 (2019) 317–324.
[11] X. Zhan, C. Li, C. Zhang, et al., Intercropping maize and soybean increases efficiency of land and fertilizer nitrogen use, a meta-analysis (2020) 107661.
[12] C. Li, E. Hoffland, T.W. Kuyper, et al., Syndromes of production in intercropping impact yield gains, J. Nature Plants 6 (6) (2020) 653–660.
[13] W. Yin, Q. Chai, C. Zhao, et al., Water utilization in intercropping: a review, Agric. Water Manag. 241 (2020) 106335.
[14] M.S. Kukal, S. Irmak, Light interactions, use and efficiency in row crop canopies under optimal growth conditions, Agric. For. Meteorol. 284 (2020) 107887.
[15] R. Zhang, Y. Mu, X. Li, et al., Response of the arbuscular mycorrhizal fungi diversity and community in maize and soybean rhizosphere soil and roots to intercropping systems with different nitrogen application rates, Sci. Total Environ. 740 (2020) 139810.
[16] Z. Cheng, L. Meng, T. Yin, et al., Changes in soil rhizobia diversity and their effects on the symbiotic efficiency of soybean intercropped with maize, Agronomy 13 (4) (2023) 997.
[17] Q. Du, L. Zhou, P. Chen, et al., Relay-intercropping soybean with maize maintains soil fertility and increases nitrogen recovery efficiency by reducing nitrogen input, The Crop Journal 8 (1) (2020) 140–152.
[18] J.G. Franco, S.R. King, A. Volder, Component crop physiology and water use efficiency in response to intercropping, Eur. J. Agron. 93 (2018) 27–39.
[19] H. Dai, R. Wang, L. Chen, et al., Effects of different micro-irrigation methods on water use and the economic benefits of an apple–soybean intercropping system, Agronomy 13 (4) (2023) 1143.
[20] M.A. Raza, H.S. Yasin, H. Gul, et al., Maize/soybean strip intercropping produces higher crop yields and saves water under semi-arid conditions, Front. Plant Sci. 13 (2022) 1006720.
[21] M.A. Raza, L. Cui, I. Khan, et al., Compact maize canopy improves radiation use efficiency and grain yield of maize/soybean relay intercropping system, Environ. Sci. Pollut. Control Ser. 28 (2021) 41135–41148.
[22] E. Mugi-Ngenga, L. Bastiaans, N.P.R. Anten, et al., The role of inter-specific competition for water in maize-legume intercropping systems in northern Tanzania, Agric. Syst. 207 (2023) 103619.
[23] M.A. Awal, H. Koshi, T. Ikeda, Radiation interception and use by maize/peanut intercrop canopy, Agric. For. Meteorol. 139 (1–2) (2006) 74–83.
[24] Z. Wang, X. Zhao, P. Wu, et al., Radiation interception and utilization by wheat/maize strip intercropping systems, Agric. For. Meteorol. 204 (2015) 58–66.
[25] A. Tabarzad, A.A. Ghaemi, S. Zand-Parsa, Extinction coefficients and radiation use efficiency of barley under different irrigation regimes and sowing dates, Agric. Water Manag. 178 (2016) 126–136.
[26] C.R. Lowe, An introduction to the concepts and technology of biosensors, Biosensors 1 (1) (1985) 3–16.
[27] L. Dong, Y. Lu, G. Lei, et al., Improve the simulation of radiation interception and distribution of the strip-intercropping system by considering the geometric light transmission, Agronomy 14 (1) (2024) 227.
[28] Z.K. Wang, P.T. Wu, X.N. Zhao, et al., Simulation of instantaneous light transmission in wheat/maize intercropping canopy in hetao region, China, Ying Yong Sheng tai xue bao= The Journal of Applied Ecology 26 (6) (2015) 1704–1710.
[29] S. Xiao, S. Fei, Q. Li, et al., The importance of using realistic 3D canopy models to calculate light interception in the field, Plant Phenomics 5 (2023) 82.
[30] Y. Wu, D. He, E. Wang, et al., Modelling soybean and maize growth and grain yield in strip intercropping systems with different row configurations, Field Crops Res. 265 (2021) 108122.
[31] G. Yang, J. Liu, C. Zhao, et al., Unmanned aerial vehicle remote sensing for field-based crop phenotyping: current status and perspectives, Front. Plant Sci. 8 (2017) 1111.

[32] N. Zendonadi dos Santos, H.P. Piepho, G.E. Condorelli, et al., High-throughput field phenotyping reveals genetic variation in photosynthetic traits in durum wheat under drought, Plant Cell Environ. 44 (9) (2021) 2858–2878.
[33] R.T. Furbank, J.A. Jimenez-Berni, B. George-Jaeggli, et al., Field crop phenomics: enabling breeding for radiation use efficiency and biomass in cereal crops, New Phytol. 223 (4) (2019) 1714–1727.
[34] Y. Liu, G. Zhang, K. Shao, et al., Segmentation of individual leaves of field grown sugar beet plant based on 3D point cloud, Agronomy 12 (4) (2022) 893.
[35] T.J. Young, T.Z. Jubery, C.N. Carley, et al., "Canopy fingerprints" for characterizing three-dimensional point cloud data of soybean canopies, Front. Plant Sci. 14 (2023) 1141153.
[36] S. Paulus, J. Dupuis, A.K. Mahlein, et al., Surface feature based classification of plant organs from 3D laserscanned point clouds for plant phenotyping, BMC Bioinf. 14 (2013) 1–12.
[37] P. Kumar, J. Connor, S. Mikiavcic, High-throughput 3D reconstruction of plant shoots for phenotyping[C], 2014 13th International Conference on Control Automation Robotics & Vision (ICARCV). IEEE (2014) 211–216.
[38] N. Harandi, B. Vandenberghe, J. Vankerschaver, et al., How to make sense of 3D representations for plant phenotyping: a compendium of processing and analysis techniques, Plant Methods 19 (1) (2023) 60.
[39] H. Sinoquet, B. Moulia, R. Bonhomme, Estimating the three-dimensional geometry of a maize crop as an input of radiation models: comparison between three-dimensional digitizing and plant profiles, Agric. For. Meteorol. 55 (3–4) (1991) 233–249.
[40] B. Zhu, F. Liu, Z. Xie, et al., Quantification of light interception within image-based 3-D reconstruction of sole and intercropped canopies over the entire growth season, Ann. Bot. 126 (4) (2020) 701–712.
[41] M. Li, P. Hu, D. He, et al., Quantification of the cumulative shading capacity in a maize–soybean intercropping system using an unmanned aerial vehicle, Plant Phenomics 5 (2023) 95.
[42] S. Xiao, H. Chai, K. Shao, et al., Image-based dynamic quantification of aboveground structure of sugar beet in field, Remote Sens. 12 (2) (2020) 269.
[43] D.J. Midmore, Agronomic modification of resource use and intercrop productivity, Field Crops Res. 34 (3–4) (1993) 357–380.
[44] F. Yang, D. Liao, X. Wu, et al., Effect of aboveground and belowground interactions on the intercrop yields in maize-soybean relay intercropping systems, Field Crops Res. 203 (2017) 16–23.
[45] G. Rana, N. Katerji, Measurement and estimation of actual evapotranspiration in the field under mediterranean climate: a review, Eur. J. Agron. 13 (2–3) (2000) 125–153.
[46] A. Rg, Crop evapotranspiration: guidelines for computing crop water requirements, FAO Irrig Drain 56 (1998) 147–151.
[47] S. Xiao, Y. Ye, S. Fei, et al., High-throughput calculation of organ-scale traits with reconstructed accurate 3D canopy structures using a UAV RGB camera with an advanced cross-circling oblique route, ISPRS J. Photogrammetry Remote Sens. 201 (2023) 104–122.
[48] H. Chen, M. Zhang, S. Xiao, et al., Quantitative analysis and planting optimization of multi-genotype sugar beet plant types based on 3D plant architecture, Comput. Electron. Agric. 225 (2024) 109231.
[49] Y. Li, C. Yu, J. Sun, et al., Nitrogen Environmental Endurance and economically-ecologically Appropriate Amount of Nitrogen Fertilizer in Faba bean/maize Intercropping System, 2008, pp. 223–227.
[50] G. Zhang, Z. Yang, S. Dong, Interspecific competitiveness affects the total biomass yield in an alfalfa and corn intercropping system, Field Crops Res. 124 (1) (2011) 66–73.
[51] T. Rahman, L. Ye, X. Liu, et al., Water use efficiency and water distribution response to different planting patterns in maize–soybean relay strip intercropping systems, Exp. Agric. 53 (2) (2017) 159–177.
[52] G. Liu, Y. Yang, W. Liu, et al., Optimized canopy structure improves maize grain yield and resource use efficiency, Food Energy Secur. 11 (2) (2022) e375.
[53] X. Liu, Y. Feng, T. Hu, et al., Enhancing ecosystem productivity and stability with increasing canopy structural complexity in global forests, Sci. Adv. 10 (20) (2024).
[54] G.B. Bonan, E.G. Patton, J.J. Finnigan, et al., Moving beyond the incorrect but useful paradigm: reevaluating big-leaf and multilayer plant canopies to model biosphere-atmosphere fluxes–a review, Agric. For. Meteorol. 306 (2021) 108435.
[55] F. Hui, J. Zhu, P. Hu, et al., Image-based dynamic quantification and high-accuracy 3D evaluation of canopy structure of plant populations, Ann. Bot. 121 (5) (2018) 1079–1088.
[56] Q. Hao, C. Huang, A review of forest aboveground biomass estimation based on remote sensing data, Chinese Journal of Plant Ecology 47 (10) (2023) 1356.
[57] D. Tian, Z.B. Yan, J.Y. Fang, Review on characteristics and main hypotheses of plant ecological stoichiometry, Chinese Journal of Plant Ecology 45 (7) (2021) 682–713.
[58] M.M. Duarte, R.A. Moral, J. Guillemot, et al., High tree diversity enhances light interception in tropical forests, J. Ecol. 109 (7) (2021) 2597–2611.
[59] O. Regaieg, T. Yin, Z. Malenovský, et al., Assessing impacts of canopy 3D structure on chlorophyll fluorescence radiance and radiative budget of deciduous forest stands using DART, Rem. Sens. Environ. 265 (2021) 112673.
[60] J. Lu, Q. Dong, G. Lan, et al., Row ratio increasing improved light distribution, photosynthetic characteristics, and yield of peanut in the maize and peanut strip intercropping system, Front. Plant Sci. 14 (2023) 1135580.
[61] T. Zhu, X. Ma, H. Guan, et al., A calculation method of phenotypic traits based on three-dimensional reconstruction of tomato canopy, Comput. Electron. Agric. 204 (2023) 107515.
[62] M. Li, D. He, P. Hu, et al., Quantifying lower crop radiation availability in strip intercropping systems via UAV-derived canopy structural models, Comput. Electron. Agric. 229 (2025) 109691.
[63] H. Kou, Z. Liao, Y. Liu, et al., Light distribution, interception and use efficiency of drip-fertigated maize-soybean strip intercropping systems under various row configuration conditions, Plant Cell Environ (2025), https://doi.org/10.1111/pce.70031.
[64] Y.Y. Ren, X.L. Wang, S.Q. Zhang, et al., Influence of spatial arrangement in maize-soybean intercropping on root growth and water use efficiency, Plant Soil 415 (1) (2017) 131–144.
[65] B. Li, Y.Y. Li, H.M. Wu, et al., Root exudates drive interspecific facilitation by enhancing nodulation and N2 fixation, Proc. Natl. Acad. Sci. 113 (23) (2016) 6496–6501.
[66] Y. Zhang, Z. Sun, Z. Su, et al., Root plasticity and interspecific complementarity improve yields and water use efficiency of maize/soybean intercropping in a water-limited condition, Field Crops Res. 282 (2022) 108523.
[67] Y. Tan, F. Hu, Q. Chai, et al., Expanding row ratio with lowered nitrogen fertilization improves system productivity of maize/pea strip intercropping, Eur. J. Agron. 113 (2020) 125986.
[68] C.L. Luo, H.X. Duan, Y.L. Wang, et al., Complementarity and competitive trade-offs enhance forage productivity, nutritive balance, land and water use, and economics in legume-grass intercropping, Field Crops Res. 319 (2024) 109642.
[69] L. Feng, M.A. Raza, J. Shi, et al., Delayed maize leaf senescence increases the land equivalent ratio of maize soybean relay intercropping system, Eur. J. Agron. 118 (2020) 126092.
[70] F. Jin, Z. Wang, H. Zhang, et al., Quantification of spatial-temporal light interception of crops in different configurations of soybean-maize strip intercropping, Front. Plant Sci. 15 (2024) 1376687.
[71] Y. Li, Q. Wang, S. Gao, et al., Vulnerability of xylem embolism in maize cultivars with different drought tolerance under water and salt stress, Agronomy 14 (3) (2024) 438.
[72] S. Stojnić, M. Suchocka, M. Benito-Garzón, et al., Variation in xylem vulnerability to embolism in European beech from geographically marginal populations, Tree Physiol. 38 (2) (2018) 173–185.
[73] D.L. Jiang, H.W. Wang, J. Jiang, et al., Correlations between characters of roots and those of aerial parts of maize in different plant type, Seed 33 (7) (2014) 94–96.
[74] H.X. Zhao, P. Zhang, Y.Y. Wang, et al., Canopy morphological changes and water use efficiency in winter wheat under different irrigation treatments, J. Integr. Agric. 19 (4) (2020) 1105–1116.
[75] L.H. Comas, T.J. Trout, K.C. DeJonge, et al., Water productivity under strategic growth stage-based deficit irrigation in maize, Agric. Water Manag. 212 (2019) 433–440.
[76] S. He, X. Li, M. Chen, et al., Excellent canopy structure in soybeans can improve their photosynthetic performance and increase yield, Agriculture 14 (10) (2024) 1783.